

## Experimental study on the shear thinning effects of viscosity index improver added lubricant by in-situ optical viscometer

Siyoul Jang\*

School of Mechanical & Automotive Engineering, Kookmin University  
861-1, Jungnung-dong, Sungbuk-gu, Seoul 136-702, Korea

(Received April 15, 2003; final revision received June 2, 2003)

### Abstract

Elastohydrodynamic lubrication (EHL) film is measured under the condition of viscosity index improver added to base oil. In-situ optical contact method using the interference principle make the measuring resolution of ~5 nm possible and enables the measuring range all over the contact area of up to ~300  $\mu\text{m}$  diameter. What is more important to the developed method by the author is that the measurement of EHL film thickness is possible in the range from 100 nm to 2  $\mu\text{m}$ , which is the regime of worst contact failures in precision machinery. Viscosity index improver (VII) is one of the major additives to the modern multigrade lubricants for the viscosity stability against temperature rise. However, it causes shear thinning effects which make the film thickness lessened very delicately at high shear rate (over  $10^5 \text{ s}^{-1}$ ) of general EHL contact regime. In order to exactly verify the VII's performance of viscosity stability at such high shear rate, it is necessary to make the measurement of EHL film thickness down to ~100 nm with fine resolution for the preliminary study of viscosity control. In this work, EHL film thickness of VII added lubricant is measured with the resolution of ~5 nm, which will give very informative design tool for the synthesis of lubricants regarding the matter of load carrying capacity at high shear rate condition.

**Keywords** : elastohydrodynamic lubrication (EHL), in-situ EHL optical interferometer (optical viscometer), viscosity index improver, shear thinning, multigrade lubricant

### 1. Introduction

Many experimental and numerical studies about elastohydrodynamic lubrication (EHL) have been performed on the assumption of Newtonian fluid. Most published formulas relating the properties such as viscosity, contact velocity, applied load, viscosity-pressure characteristics and elastic modulus in both experimental and numerical investigations predict film thicknesses with the assumption of Newtonian fluid by Hamrock (1994). However, recently developed lubricants show very non-linear behaviors of viscosity-shear rate especially in EHL regime, where high concentrated pressure (1.0 GPa), thin film thickness and large contact velocity (over  $10^5 \text{ s}^{-1}$ ) occur over the contact area. This is the reason that many VII's additives for better performance of lubricant against temperature rise in EHL regime make the lubricant film unpredictively thinner at high shear rate.

Many developed empirical formula for lubricant film thickness in EHL regime do not very frequently match

with the experimental investigations especially to viscosity index improver (VII) added lubricant in the work by Johnson, *et al.* (1991). In general, VII additives have large molecular weights (*i.e.* polyalkylmethacrylate, PAMA) ranging from 610,000 to 3,200,000 with long chained structure. They change the molecular structures into aligning shapes along the contact direction on the solid surfaces when the two contacting surfaces are sheared. This behavior is not accounted in most of continuum numerical investigations for predicting the central film thickness of an oil-lubricated contact by Newtonian fluid in elastohydrodynamic lubrication by many previous works, Evans (1986), Ostensen (1995).

In-situ EHL optical interferometric technology (that is, optical viscometer) for measuring the film thickness is very useful method in the investigations of rheological properties of lubricant at high shear rate and high applied load. It simulates most of contact geometries, materials and lubrication conditions by changing the contact curvatures of radius, equivalent of elastic modulus, starvation or flooded boundary conditions. In particular, it can provide the visualization of the EHL film thickness images all over the contact area in the studies by Bair (1995), Williamson

\*Corresponding author: jangs@kookmin.ac.kr  
© 2003 by The Korean Society of Rheology

(1995) and Smeeth *et al.* (1995). Another great advantage of this in-situ EHL optical measuring technology is that it can test various contact velocities (or shear strain rates) up to  $10^8 \text{ s}^{-1}$ , which most severe contact environments in precision elements of machinery have.

Digital image processing technology by Krupka *et al.* (1997) also enhances the performance of in-situ optical EHL interferometric method by giving consistent and objective interpretation tool of measured film thickness over the contact area with very fine resolution of  $\sim 10 \text{ nm}$ . Without the developed technology, only central and minimum film thickness might be concerned, which makes the interpretation of measure film thickness by naked eye much biased to the observers experiences.

In this work, minute changes of EHL film thickness with VII added condition are investigated for the preliminary study of lubricant synthesis design with various kinds of contact velocities and loads down to  $\sim 100 \text{ nm}$  of EHL film thickness. The investigations are performed by in-situ EHL optical interferometric apparatus and image processing technology with less than  $\sim 5 \text{ nm}$  scale of film thickness previously developed by the author.

## 2. Apparent viscosity change by the viscosity index improver

Viscosity index improver in the multigrade lubricant is used against the rapid drop of viscosity at working temperature rising up to  $150^\circ\text{C}$ . Many precision contacts of mechanical elements such as cam-tappet in automobile engine and ball-race in precision rolling contact bearings have severe contact behaviors of elastohydrodynamic lubrication regime which have both high shear rate modes over  $10^5 \text{ s}^{-1}$  and high pressure over  $1.0 \text{ GPa}$  in general. However, the viscosity stability by long chained polymeric molecular structure of VII against temperature rise is delicately influenced by such high shear rate with thin fluid film ( $\sim 0.1 \mu\text{m}$ ), which is common working condition of precision machinery. At such high shear rate where high concentrated normal pressure on the contact area is accompanied, the polymeric molecules are aligned along the sliding direction and subsequently the apparent viscosity (or shear resistance) is lessened in thin film status under high normal pressure. This is the reason that the load carrying capacity of lubricant with VII containing long chained polymeric molecules is far smaller than pure base oil under the condition of the same applied load as shown in the work by Bird *et al.* (1987) and Harris (1977).

The fluid film pressure in the contact area is described by the following Reynolds equation with respect of continuum mechanics by Hamrock (1994).

$$\frac{\partial}{\partial x} \left( \frac{\rho h^3}{12\eta} \frac{\partial p}{\partial x} \right) + \frac{\partial}{\partial y} \left( \frac{\rho h^3}{12\eta} \frac{\partial p}{\partial y} \right) - u \frac{\partial(\rho h)}{\partial x} = 0 \quad (1)$$

where the viscosity  $\eta = f\left(\frac{dy}{dt}, p\right)$  has the functions of shear rate and applied pressure.

The load capacity by the fluid film pressure is computed by the summation of pressure over the contact area as shown below.

$$W = \int_A p(x,y) dx dy \quad (2)$$

Conventional viscometer like cone-plate rheometry system, Fig. 1 measures the viscosity by sensing the shear resistance with rotating two thin-separated plates ( $\sim 1 \text{ mm}$ ). This measurement can easily verify the viscosity changes according to shear rates less than  $\sim 10^5 \text{ s}^{-1}$ . However, the measurement range of shear strain rate by cone-plate viscometer is still much lower than that of actual contacts of precision mechanical elements and does not give informative design parameters for the blending of lubricant. What is less, it measures the viscosity values only under the condition of atmospheric pressure where the true viscosity performance of lubricant cannot be verified at all under the real contact environment.

Viscosity variations are measured in this study according to cone-plate viscometer (Paar-Physica UM) where the testing range of shear strain rate is possible up to  $10^5 \text{ s}^{-1}$  at most. This is the range far below shear rate in the real contacts of precision mechanical elements and it provides only the results of atmospheric pressure, while most precision mechanical elements undergo pressures over  $1.0 \text{ GPa}$  and shear strain rates over  $10^5 \text{ s}^{-1}$ , respectively. Viscosity changes by the additions of VII to base oil are measured by cone and plate viscometer as shown in Fig. 2. Addition of VII to base oil makes the lubricant more viscous, but the viscosity of each case decreases as the shear rate increases. The higher portion of VII in the blended lubricant (multigrade lubricant), the more rapid drop of viscosity as the shear rates increase. This is the general tendency when VII is added even under atmospheric pressure. Further increase of shear rate in cone and plate viscometer for the viscosity measurement of EHL regime needs much thinner contact of  $\sim \mu\text{m}$  gap between cone and plate or increase rotational

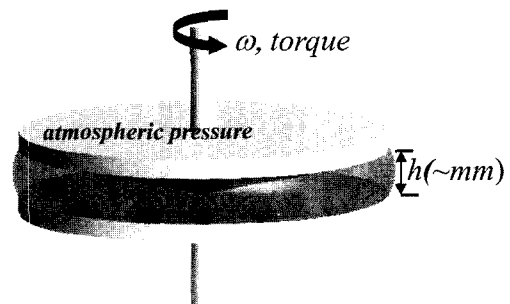
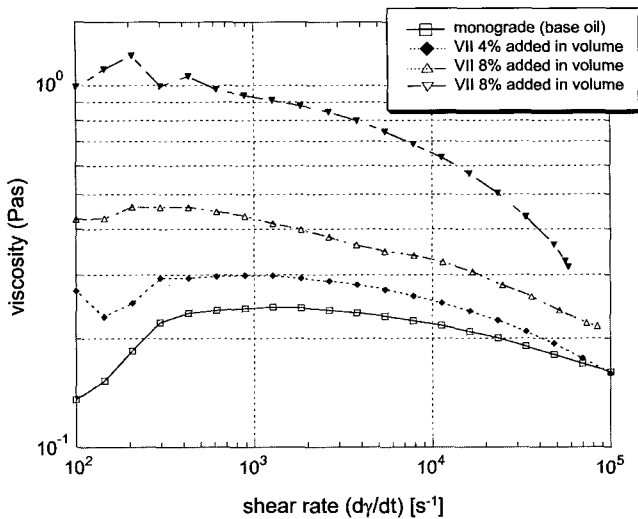


Fig. 1. Viscosity measurement according to the variation of shear strain rate by cone and plate viscometer (Paar-Physica UM).



**Fig. 2.** Viscosity variations according to portion of the viscosity index improver by cone and plate viscometer (Paar-Physica UM) up to  $10^5 \text{ s}^{-1}$  of shear strain rate.

speed of cone. However, this is not simple problem with the respects of parallel control of  $\sim \mu\text{m}$  gap between cone and plate which might has a relatively large contact area of  $\sim 2000 \text{ mm}^2$  scale as well as rotational inertia control of tested lubricant by dissipated effect.

In order to verify the performance of long chained polymeric VII under the condition of high shear rate and high pressure for the high-performance lubricant design, it is necessary to make the precision measurement of contact film thickness, contact velocity and applied load at the same time. Although the measurement of contact velocity and applied load are easily obtainable by sensing the speed of driving motor and the kinematic contact geometry, respectively, the measurement of film thickness needs much precision for fine resolution in both normal and shearing orientations of contact.

In-situ EHL optical interferometric method makes it possible to make the measurement of area size of contact spot as well as film thickness ranging from 100 nm to  $2 \mu\text{m}$  with  $\sim 5 \text{ nm}$  resolution over the contact area. The measured contact size provides the information of applied load, material modulus and contact geometry, because the kinematic geometry of in-situ EHL contact feature realizes the contact behaviors in precision elements of machinery. The viscosity characteristics to any shear rates under high pressure up to  $\sim 1.5 \text{ GPa}$  can be verified by the captured interferometric image of EHL film thickness in fine resolution only with the measurement of rotational torque. The pattern of EHL film thickness also provides informative pressure-viscosity characteristics of tested lubricant that cannot be obtained by other methods with such simple way. Many other advantages of in-situ EHL optical viscometer over the conventional high shear rate viscometers are the followings: 1) Conventional high shear rate viscometer oper-

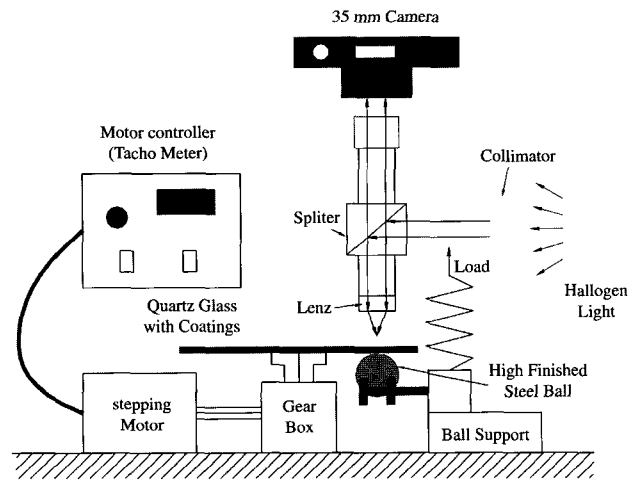


**Fig. 3.** Schematic diagram of in-situ EHD optical interferometer (optical viscometer) for film measurement.

ates only at atmospheric pressure which cannot consider the high concentrated effect of pressure. 2) It generates heat and it is difficult to determine true oil temperature. 3) In real contact of machinery such as cam-tappet contact, the lubricant undergoes intermittent shear once per revolution of the cam, while the conventional high shear viscometer is subjected to prolonged shearing during the test.

In this experimental work of load carrying capacity of VII added lubricants, in-situ EHL apparatus for measuring the interference images of EHL film thickness with VII added lubricants is developed as well as color-film thickness chart in terms of CIE  $L^*a^*b^*$  under the condition of white incident light are made. The developed system can make the measurement of EHL film thickness with  $\sim 5 \text{ nm}$  resolution. The performance of the optical interference method is very strongly dependent on the coating layer on the transparent glass whose thickness are coated with around 10 nm thickness of Cr layer on the highly transparent glass of 150 mm diameter (Fig. 3). White light is fil-

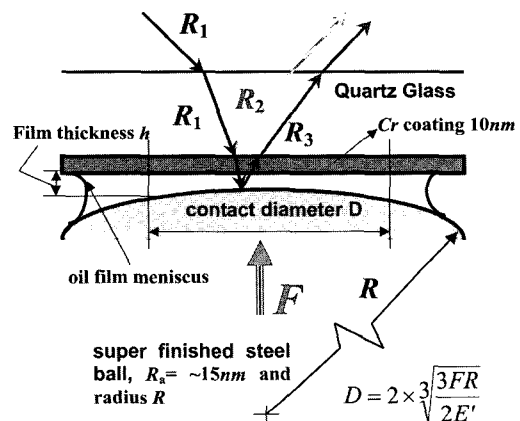


**Fig. 4.** Reflected beams on Cr coating surface (half mirror) and steel ball.

tered with day light filter that can pass all frequencies of visible colors and fine finished steel ball of 25 mm diameter with the roughness of  $R_a$ , 15 nm scale are used so that the incident light can be reflected by 25% of after the Cr layer in order to get the most distinct resolution without any noise (Fig. 4). Schematic diagram of the developed device and the mechanism of incident light reflection are shown in Fig. 3 and 4. The elastic modulus and Poisson's ratios of glass and ball are  $E_b=207\times 10^9$  N/m<sup>2</sup>,  $E_d=76\times 10^9$  N/m<sup>2</sup>,  $\nu_b=0.30$ ,  $\nu_d=0.25$ , respectively.

### 3. EHL film thickness-color chart by image processing method under white incident light

One of the powerful methods in color decomposition is CIE 1976  $L^*a^*b^*$  decomposition technique that uses three independent components  $L^*$ ,  $a^*$  and  $b^*$  in order to reproduce digitally formatted colors in the computer. CIE  $L^*a^*b^*$  decomposition of interferogram colors in EHL film thickness image can provide perceptual uniformity, device independence and color difference equation for EHL film thickness. The tristimulus values of  $X_n$ ,  $Y_n$  and  $Z_n$  for reference white incident light is computed after the red, green and blue components (RGB) of white light are decomposed.

Every pixel in the color interferogram outside of Hertzian contact circle as shown in Fig. 5 is decomposed into RGB values, which are subsequently converted into  $L^*$ ,  $a^*$  and  $b^*$  values for the calibration of film thickness (Fig. 6). The film thickness outside of Hertzian contact area is obtainable by numerical computation of Hertzian contact theory. The EHL film thickness-color chart is then obtained by matching the  $L^*$ ,  $a^*$  and  $b^*$  values with the gap between steel ball and glass plate from Hertzian contact theory. (Fig. 7) In this experimental study, EHL film thickness can be fully investigated with the developed chart in the range from 100 nm to 700 nm all over the contact area, which cannot be accessible with other measuring systems such as capacitance gap sensor, infrared light and any other spectrometers measuring only single large spot (~mm diameter size) in the Hertzian contact area.

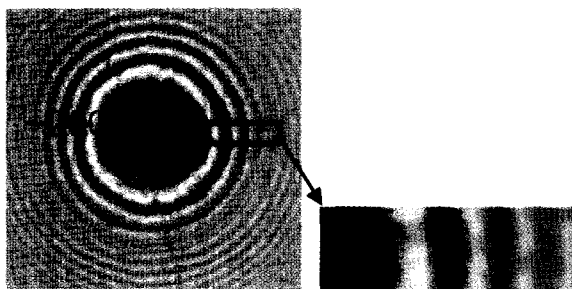


Fig. 5. Interferogram of white incident light with 10 N static load and color changes at the fringe boundaries as the film thickness changes.

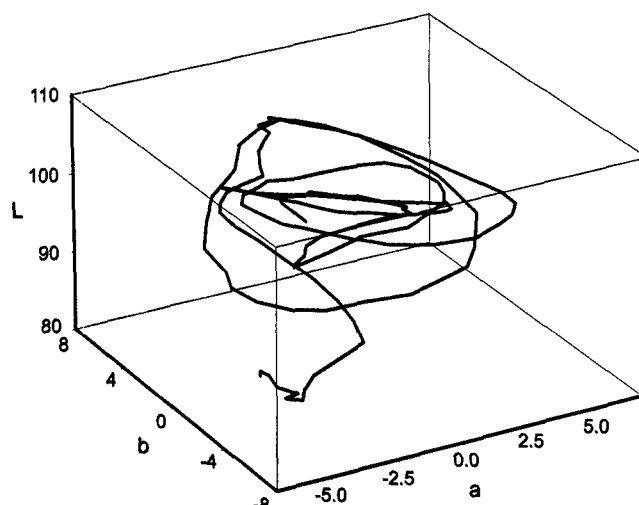


Fig. 6. Spatial color coordinates of  $L^*a^*b^*$  by white incident light in the range of 100~700 nm of EHL film thickness.

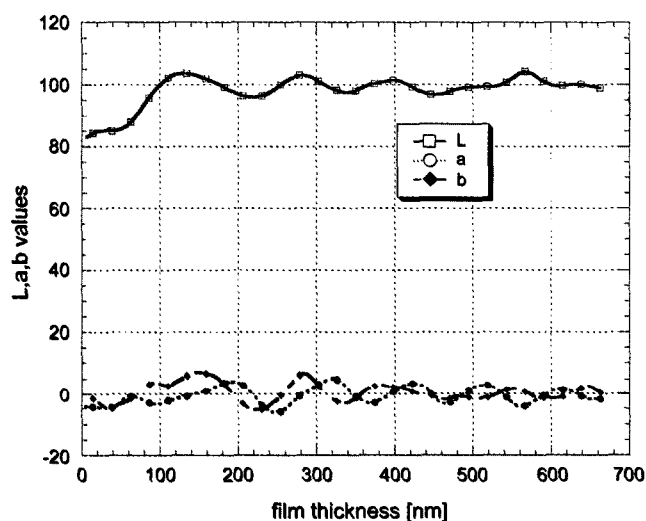


Fig. 7. Film thickness-color chart for EHL contact by white incident light.

Once the EHL film thickness-color chart is made as in Fig. 7, every  $L^*a^*b^*$  formatted pixel in the captured color interferogram of EHL film thickness is compared with the chart. In order for the selected pixel to get the nearest value to the computed  $L^*a^*b^*$  chart, sweeping all over the captured pixels with the minimization of color difference  $\Delta E_{ab}^*$  is performed by the following color difference equation by Krupka *et al.* (1997).

$$\Delta E_{ab}^* = [(\Delta L^*)^2 + (\Delta a^*)^2 + (\Delta b^*)^2]^{1/2} \quad (3)$$

With both the developed experimental apparatus and the image processing technology, minute variations of EHL film thickness less than ~5 nm film thickness according the addition of VII to base oil can be detectable at high shear rate over  $10^5$  s<sup>-1</sup> with consistency and objectivity.

#### 4. Results

The viscosity of the lubricant under atmospheric pressure, ambient temperature 20°C and  $\sim 10^2 \text{ s}^{-1}$  shear rate is measured around  $\sim 1.0 \text{ Pas}$  by cone and plate viscometer (Fig. 2). Under the condition of ambient temperature and pressure ( $\sim 10^{-4} \text{ GPa}$ ) with low shear rate around  $\sim 10^2 \text{ s}^{-1}$ , the viscosity of the blended lubricant has higher values as the portion of VII in the base oil. This is taken for granted because VII is much more viscous than base oil in general. However, higher shear rate over  $10^5 \text{ s}^{-1}$  makes the viscosity decrease rapidly as more VII is added to the base oil. That is, higher tendency of shear thinning behavior becomes with more VII added to base oil even under ambient temperature. Under the contact of high normal stress over 0.5 GPa and high shear rate over  $10^5 \text{ s}^{-1}$  where EHL contact occurs, shear thinning effect is more vivid than the tested results by cone and plate viscometer.

The developed in-situ EHL optical interferometry of EHL contact can verify the shear thinning behaviors under various contact loads and velocities by capturing the images of contact spot. In this work, the calibration data for the range of image processed film thickness is set up into EHL film thickness-color charts (Fig. 6 and 7). According to the obtained EHL film thickness-color charts, the film thickness can be digitally processed in the range of 100 nm~700 nm with the resolution of  $\sim 5 \text{ nm}$  over the contact area depending on the noise in the captured images and the incident light. The captured optical interferogram images of EHL film thickness over the Hertzian contact area are converted into digitally formatted pixel such as CIE  $L^*a^*b^*$  and compared with EHL film thickness-color chart pixel by pixel. The film thickness on each pixel is

**Table 1.** Properties of tested base oil and viscosity index improver

test items	method	base oil	VII
Density@15°C	ASTM D 1298	0.8897	0.8943
Color (ASTM)	ASTM D 1500	L1.5	L0.5
Kin. Vis 40°C (cSt)	ASTM D 445	95.09	—
Kin. Vis 100°C (cSt)	ASTM D 445	10.85	534
Pour Point °C	ASTM D 97	-15	—
Flash Point °C	ASTM D 92	242	—
TBN, mgKOH/g	ASTM D 2896	—	—

**Table 2.** Selected four cases out of 55 tested conditions in in-situ EHL interferometer

selected test cases	lubricant	applied load [N]	contact velocity [m/s]
case I	base oil	10N	0.08233 m/s
case II	base oil	15N	0.0382 m/s
case III	base oil+VII 18%	10N	0.06586 m/s
case IV	base oil+VII 18%	15N	0.06586 m/s

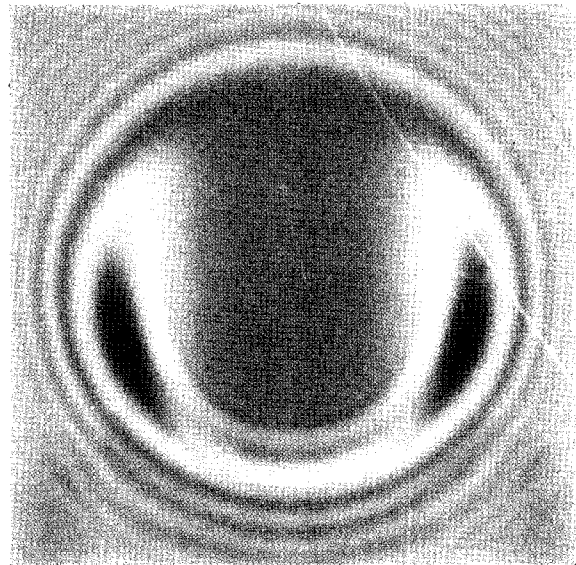


**Fig. 8.** Interferometric image of base oil under the load of 10N and rolling speed of 0.08233 m/s (Case I).

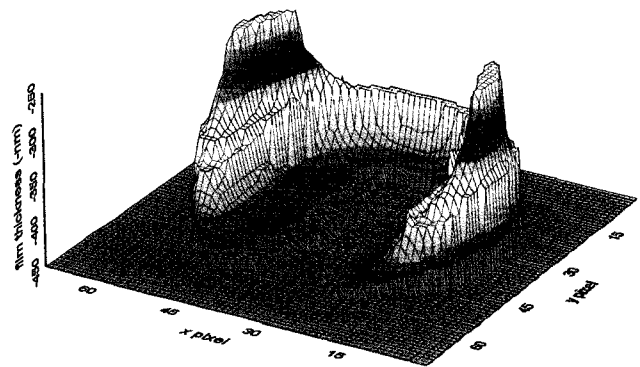


**Fig. 9.** Image processed film thickness of base oil under the load of 10N and rolling speed of 0.08233 m/s (Case I).

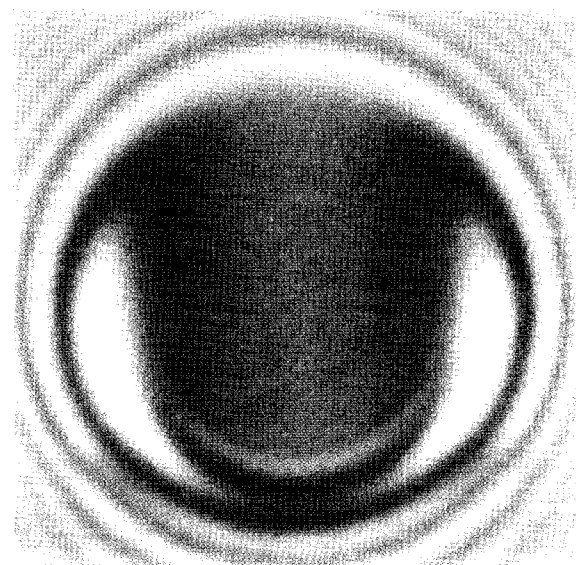


**Fig. 10.** Interferometric image of base oil under the load of 15N and rolling speed of 0.03820 m/s (Case II).

then obtained all over the contact area if it is in the range of 100 nm~700 nm.

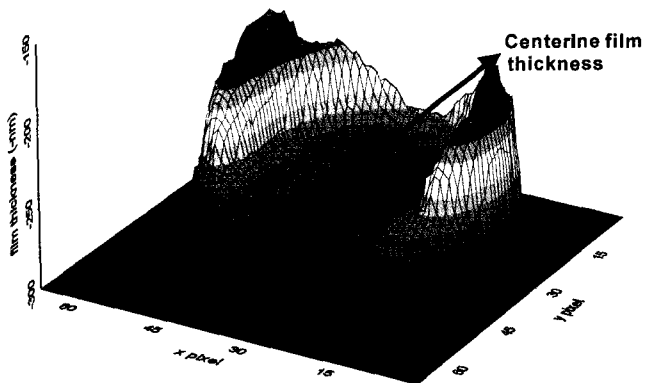


Fig. 11. Image processed film thickness of base oil under the load of 15N and rolling speed of 0.03820 m/s (Case II).

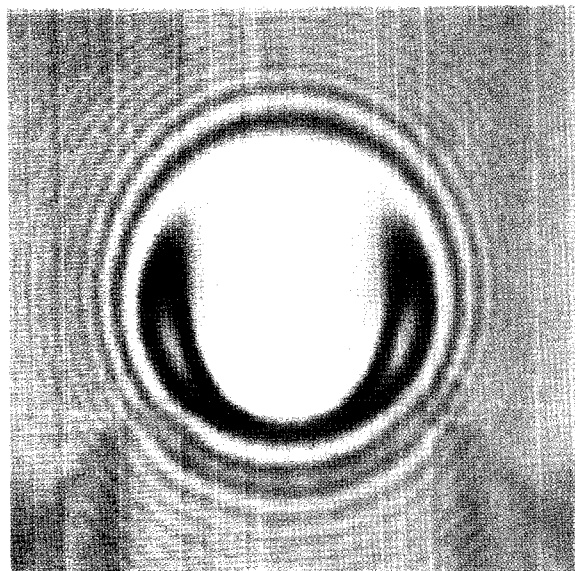


Fig. 12. Interferometric image of VII added lubricant (18%) under the load of 10N and rolling speed of 0.06586 m/s (Case III).

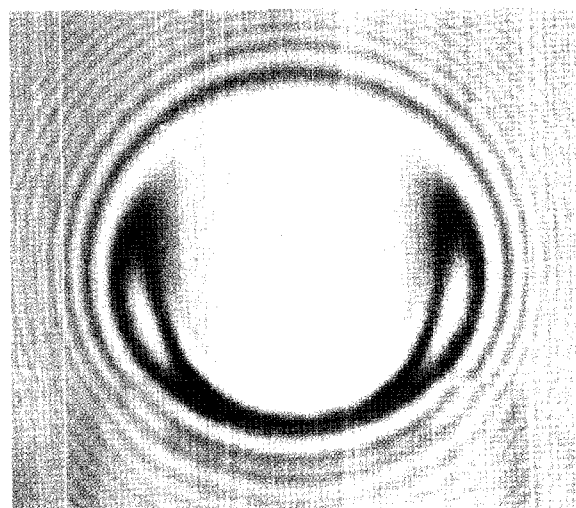


Fig. 14. Interferometric image of VII added lubricant (18%) under the load of 15N and rolling speed of 0.06586 m/s (Case IV).

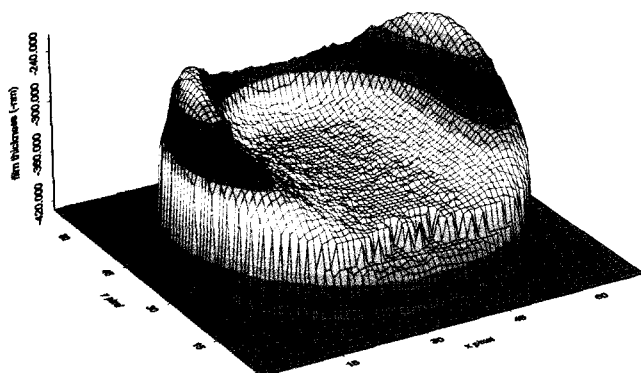


Fig. 13. Image processed film thickness of VII added lubricant (18%) under the load of 10N and rolling speed of 0.06586 m/s (Case III).

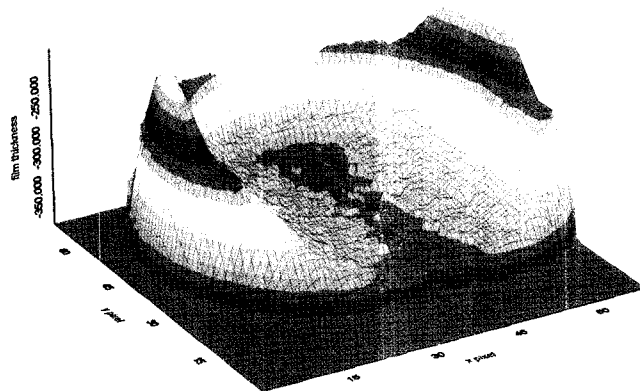


Fig. 15. Image processed film thickness of VII added lubricant (18%) under the load of 15N and rolling speed of 0.06586m/s (Case IV).

The developed image processing method is applied to the cases of VII (Table 1) effects on the load carrying performances by changing applied loads and rolling contact velocities. Delicate changes in EHL film thickness indicated by many numerical studies that cannot be investigated with other types of viscometer like con-plate viscometer are aimed to be verified by both the developed image processing method and the in-situ EHL optical interferometry. Theoretical results by Hamrock (1995) show that higher rolling contact velocity and lower applied load make the EHL film thickness thicker as long as the tested lubricant is regarded as Newtonian fluid.

Four cases (Table 2) are selected out of 55 tested results with base oil and blended VII lubricant by changing contact loads and velocities. Normal contact loads of 10N ( $P_h=0.58$  GPa,  $a=92.58$   $\mu\text{m}$ ) to 15 N ( $P_h=0.64$  GPa,  $a=105.98$   $\mu\text{m}$ ) are applied and rolling contact velocities of from 0.15 m/s to 0.015 m/s are tested, respectively. Regard-

ing the cases of base oil (monograde oil), the EHL film thickness fully takes the principle from theoretical investigations that high load and low contact velocity make the fluid film thickness thin. Film thickness of monograde oil with 10N load and 0.08233 m/s contact velocity is obtained in Fig. 8 and 9 (Case I). In case I, the minimum film thickness is around ~250 nm. Higher load and lower contact velocity (10N, 0.03820 m/s, case II) are applied to monograde oil to compare with the previous case I. Case II (Fig. 10 and 11) give minimum film thickness around ~150 nm thinner by ~100 nm than case I. These experimental results agree well with theoretical studies by many other previous researches by the works, Greenwood (1988), Hamrock (1994), Evans *et al.* (1986).

EHL film thicknesses of VII added lubricant are also measured in the same way. Contact load of 10N and rolling contact velocity of 0.06586 m/s (case III), and higher con-

tact load (15N) and same rolling contact velocity of 0.06586 m/s (case IV) are tested. Case III gives minimum film thickness of 240 nm (Fig. 12 and 13), while case IV (Fig. 14 and 15) does minimum film thickness of 200 nm. All the images of measured film thicknesses are digitally processed with 5 nm resolution by the developed technology in this work and the capability to verify the magnitude of film thickness is shown in Fig. 16 that is the centerline film thickness of Fig. 11 (Case II).

We also expand the experimental ranges of contact load and velocities (Fig. 17) for Case I, II, III and IV. The load capacities of monograde oil (case I and II) are higher than those of VII added lubricant (case III and IV) under the same contact condition by ranging from ~10 nm to ~40 nm of film thickness scale. Without the developed image processing technology of fine resolution (~5 nm) for EHL film interferogram, these finding that load carrying capacity minutely changes at high shear rate (contact velocity/measured minimum film thickness in the contact area) over  $10^5$  s<sup>-1</sup> under VII added condition cannot be verified at all.

### 5. Conclusion

In this work, optical interferometric measurement of EHL film thickness over the contact area is applied for the verification of load carrying performances of VII added lubricants, because it is possible only with fine resolution of length measurement of ~5 nm scale. Theoretically, higher rolling contact velocity under the same applied load makes the EHL film thickness thicker for Newtonian lubricant without any exemption. However, for shear thinning lubricant such as VII blended lubricant, higher contact velocity under the same applied load makes the EHL film thickness delicately thinner comparing to that of Newtonian lubricant. Therefore, minute changes of EHL film thickness due to VII addition to base oil should be verified under various contact velocities and applied loads in order to find out the VII roles in synthesized lubricant.

With the developed image processing technology for EHL film thickness and in-situ measurement apparatus by the author, minute change of load carrying performance up to ~5 nm in film thickness over the contact area can be verified for any kind of lubricants if it is under EHL contact regime. The load carrying capacities of some VII synthesized lubricant are tested and compared with Newtonian lubricant of base oil and it is found that the tested results agree well with theoretical tendencies.

### Acknowledgement

This work was supported by grant No. 2000-1-30400-005-3 from the Basic Research Program of the Korea Science & Engineering Foundation.

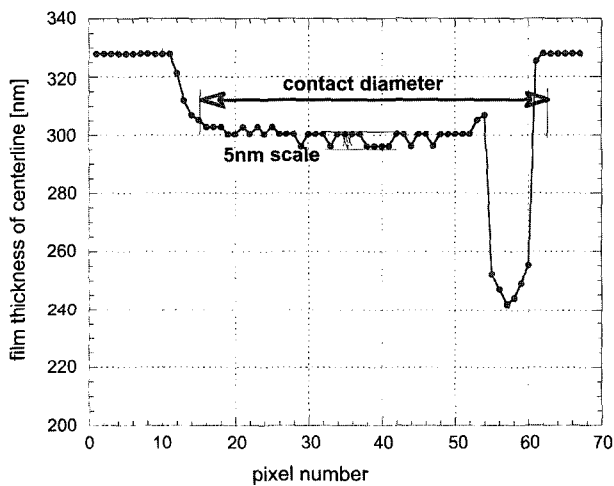


Fig. 16. Centerline film thickness of base oil under the load of 15N and rolling speed of 0.03820 m/s (Case II, Fig. 11).

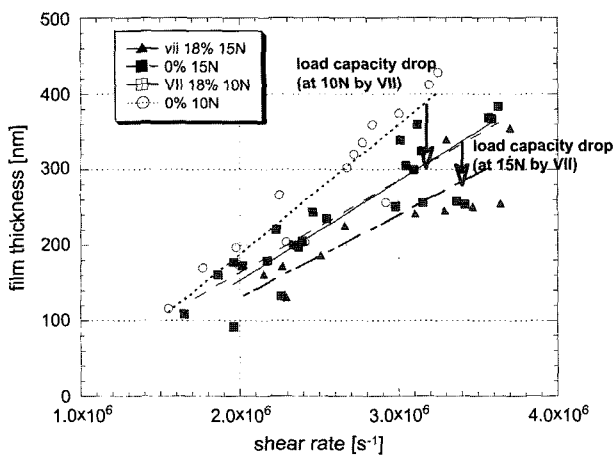


Fig. 17. Minimum film thickness variations by changing applied loads, contact velocities and VII portion in base oil (Each line is linearly curve-fitted for the same loading condition and lubricant.)

## References

- Bair, S., 1995, Elastohydrodynamic film forming with shear thinning liquids, *J. of Tribology*, **120**, 173-178.
- Bird, B., R. Armstrong and O. Hassager, 1987, Dynamics of polymeric liquids, John Wiley & Sons, New York.
- Evans, C. R. and K. L. Johnson, 1986, The rheological properties of elastohydrodynamic lubricants, *Proc. Instn. Mech. Engrs.* **200**(C5), 303-312-17.
- Greenwood, J. A., 1988, Film thickness in circular elastohydrodynamic contacts, *Proc. Instn. Mech. Engrs.* **202**(C1), 11-17.
- Greenwood, J. A. and J. J. Kauslarich, 1997, Elastohydrodynamic film thickness for shear-thinning lubricants, *Proc. Instn. Mech. Engrs.*, **212**, Part J.
- Hamrock, B. J., 1994, Fundamentals of Fluid Film Lubrication, McGraw-Hill.
- Harris, J., 1977, Rheology and non-newtonian flow, Longman, New York.
- Johnston, G. J., R. Wayte and H. A. Spikes, 1991, The measurement and study of very thin lubricant films in concentrated contact, *Tribology Transactions* **34**, 187-194.
- Krupka, M. *et al.*, 1997, Elastohydrodynamic lubrication film shape—comparison between experimental and theoretical results, tribology for energy conservation, Elsevier, Amsterdam.
- Ostensen, J. O., 1995, Prediction of film thickness in an elastohydrodynamic point contact lubricated with a viscosity index improved base oil, *Proc. Instn. Mech. Engrs.* **209**, 235-242.
- Smeeth, M., P. M. Cann and H. A. Spikes, 1995, Measurement of elastohydrodynamic film formation in rolling contacts at very high pressures, Lubricants and Lubrication, edited by Dowson, D., 497-502, Elsevier Science.
- Taylor, R. I., 1997, Engine friction: the influence of lubricant rheology, *Proc. Instn. Mech. Engrs.* **211**, Part J.
- Williamson, B. P., 1995, An optical study of grease rheology in an elastohydrodynamic point contact under fully flooded and starvation conditions, *Proc. Instn. Mech. Engrs.* **209**, 63-74.